



Minerva Access is the Institutional Repository of The University of Melbourne

Author/s:

Schwartz, BD;Coster, MJ;Skinner-Adams, TS;Andrews, KT;White, JM;Davis, RA

Title:

Synthesis and antiplasmodial evaluation of analogues based on the tricyclic core of thiaplakortones A-D

Date:

2015-09-01

Citation:

Schwartz, B. D., Coster, M. J., Skinner-Adams, T. S., Andrews, K. T., White, J. M. & Davis, R. A. (2015). Synthesis and antiplasmodial evaluation of analogues based on the tricyclic core of thiaplakortones A-D. *Marine Drugs*, 13 (9), pp.5784-5795. <https://doi.org/10.3390/md13095784>.

Persistent Link:

<https://hdl.handle.net/11343/257783>

License:

[CC BY](#)

Article

Synthesis and Antiplasmodial Evaluation of Analogues Based on the Tricyclic Core of Thiaplakortones A–D

Brett D. Schwartz ¹, Mark J. Coster ¹, Tina S. Skinner-Adams ¹, Katherine T. Andrews ¹, Jonathan M. White ² and Rohan A. Davis ^{1,*}

¹ Eskitis Institute for Drug Discovery, Griffith University, Nathan, Qld 4111, Australia; E-Mails: b.schwartz@griffith.edu.au (B.D.S.); m.coster@griffith.edu.au (M.J.C.); t.skinner-adams@griffith.edu.au (T.S.S.); k.andrews@griffith.edu.au (K.T.A.)

² School of Chemistry and Bio21 Institute, University of Melbourne, Parkville, Vic 3052, Australia; E-Mail: whitejm@unimelb.edu.au

* Author to whom correspondence should be addressed; E-Mail: r.davis@griffith.edu.au; Tel.: +61-7-3735-6043; Fax: +61-7-3735-6001.

Academic Editor: Sylvia Urban

Received: 14 August 2015 / Accepted: 7 September 2015 / Published: 15 September 2015

Abstract: Six regioisomers associated with the tricyclic core of thiaplakortones A–D have been synthesized. Reaction of 1*H*-indole-4,7-dione and 1-tosyl-1*H*-indole-4,7-dione with 2-aminoethanesulfinic acid afforded a regioisomeric series, which was subsequently deprotected and oxidized to yield the tricyclic core scaffolds present in the thiaplakortones. All compounds were fully characterized using NMR and MS data. A single crystal X-ray structure was obtained on one of the *N*-tosyl derivatives. All compounds were screened for *in vitro* antiplasmodial activity against chloroquine-sensitive (3D7) and multidrug-resistant (Dd2) *Plasmodium falciparum* parasite lines. Several analogues displayed potent inhibition of *P. falciparum* growth (IC₅₀ < 500 nM) but only moderate selectivity for *P. falciparum* versus human neonatal foreskin fibroblast cells.

Keywords: synthesis; thiaplakortone; regioisomer; tricyclic; natural product scaffold; X-ray; crystal; *Plasmodium falciparum*; antiplasmodial; cytotoxicity

1. Introduction

The marine natural products, thiaplakortones A–D (**1–4**), were first reported in 2013 as part of a Medicines for Malaria Venture sponsored research project that aimed to discover new antiplasmodial agents from nature (Figure 1) [1]. These unique thiazine-derived secondary metabolites were obtained from the organic extract from the Great Barrier Reef sponge *Plakortis lita*, and all were shown to inhibit the *in vitro* growth of *Plasmodium falciparum*. Thiaplakortone A (**1**) was the most active with *in vitro* IC₅₀ values of 6.6 and 51 nM against multidrug-resistant (Dd2) and chloroquine-sensitive (3D7) *P. falciparum* lines, respectively [1]. Due to supply issues initially curtailing *in vivo* malaria studies, total syntheses of thiaplakortones A and B were undertaken and the first total synthesis of **1** and **2**, along with a series of mono- and di-methyl analogues (**5–7**) was subsequently reported and some preliminary structure-activity relationships (SAR) ascertained (Figure 1) [2]. While *in vivo* toxicity effects for several of the synthetic compounds indicated potential liabilities associated with this structure class, the limited number of analogues investigated made it difficult to assess their true potential as antiplasmodial leads [2]. In order to more thoroughly explore this compound class a larger analogue library based on the thiaplakortone A scaffold was recently undertaken and reported [3]. This 38-membered library consisted of a series of amide and urea analogues based on the thiaplakortone A natural product scaffold. Several analogues showed potent *in vitro* *P. falciparum* growth inhibition (IC₅₀ < 500 nM) and good selectivity for *P. falciparum* versus human neonatal foreskin fibroblast (NFF) cells (selectivity index >100) [3]. Furthermore, analogues **8** and **9** displayed good metabolic stability and solubility, and when administered subcutaneously to mice plasma concentrations remained >0.2 μM for 8 h. Analogues **8** and **9** were also well tolerated in mice after subcutaneous administration of 32 mg/kg twice daily for 4 d. In addition, using this dosing protocol blood stage *P. berghei* parasitemia was suppressed by 52% for **8** and 26% for **9**, relative to controls [3]. In order to further investigate the thiaplakortone core, we have recently undertaken synthetic studies that resulted in the removal of the ethylamine side-chain present in thiaplakortones A and B in order to determine the biological implications of the –CH₂CH₂NH₂ moiety. Herein we report the total synthesis of several side-chain truncated regioisomers associated with the tricyclic core of thiaplakortones A–D, along with their *in vitro* antiplasmodial activity and mammalian cell toxicity.

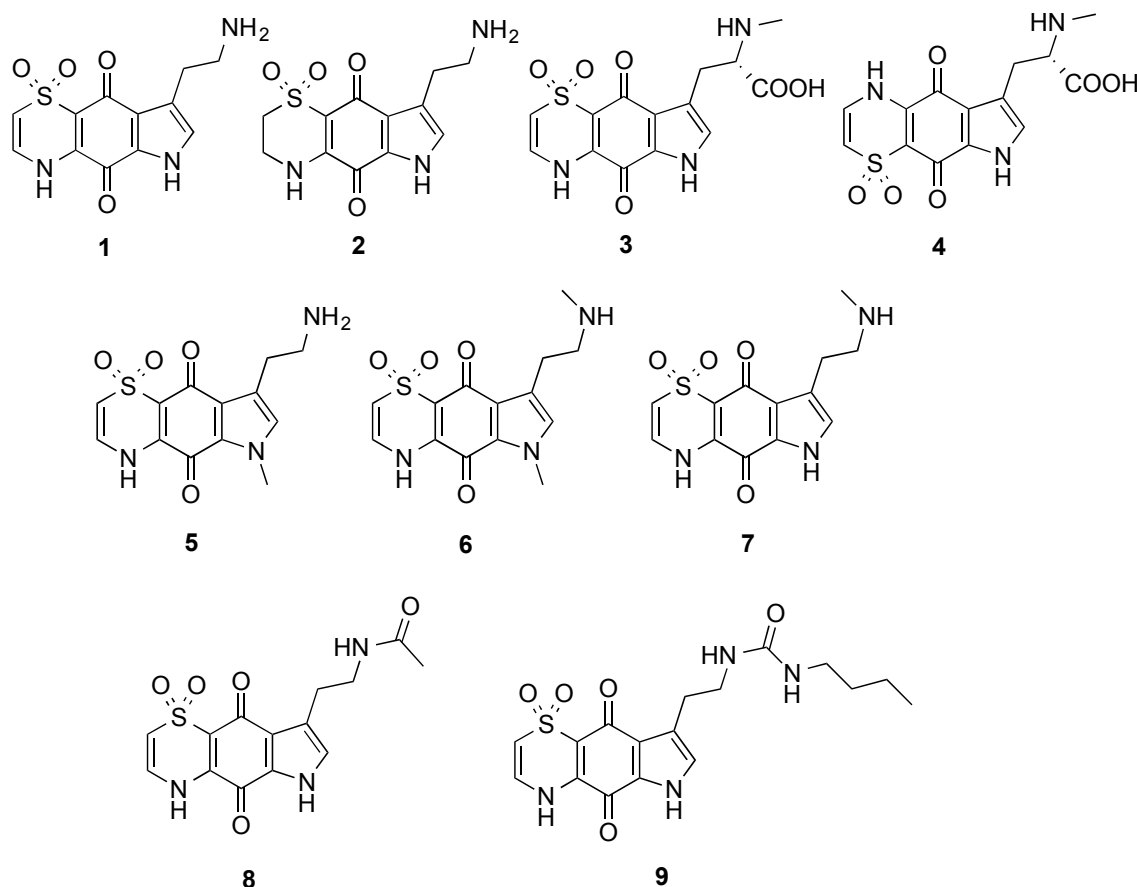


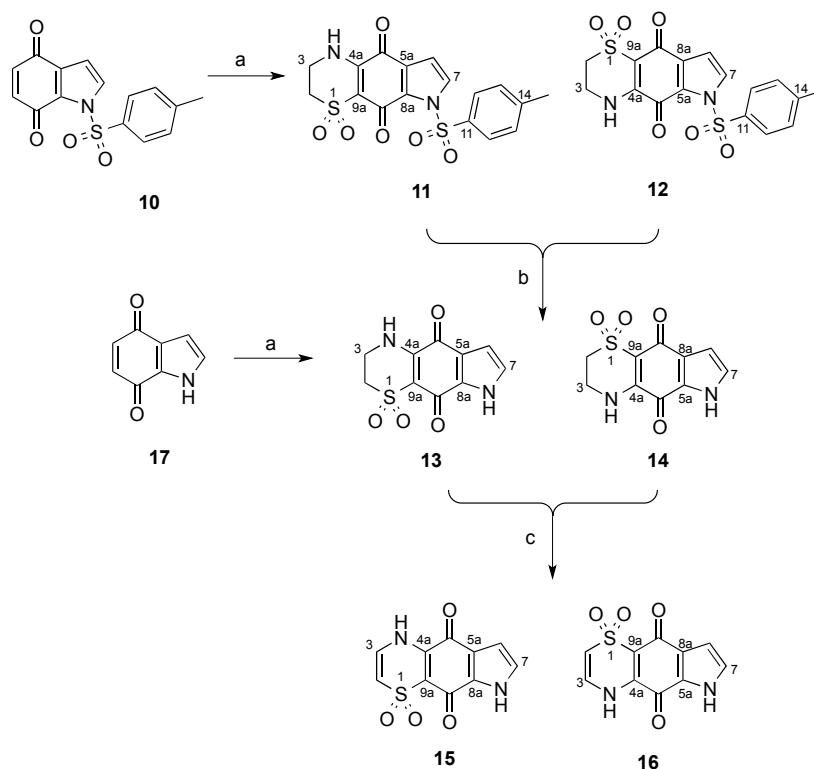
Figure 1. Chemical structures of the natural products thiaplakortones A–D (1–4) and some of the previously synthesized thiaplakortone A analogues (5–9).

2. Results and Discussion

2.1. Chemistry

The synthesis of the tricyclic core thiaplakortone isomers **11**–**16** commenced with the generation of 1-tosyl-1*H*-indole-4,7-dione (**10**), which was accessible via known procedures (Scheme 1) [4–6]. Condensation of **10** with 2-aminoethanesulfinic acid [2,7] furnished the regiomeric tricyclic systems **11** and **12** in an 11 to 1 ratio (Scheme 1). Separation of this mixture was not possible by silica flash chromatography however reversed-phase C₁₈ HPLC (MeOH–H₂O–0.1%TFA) enabled separation of the two regioisomers. Confirmation of the chemical structures of **11** and **12** was supported following extensive 1D and 2D NMR data analysis.

Furthermore, a crystal suitable for X-ray analysis was obtained on the major regioisomer **11** (Figure 2) confirming the NMR-assigned structure and establishing the regiochemistry of subsequent compounds in the tricyclic series. Of note, compound **11** crystallized with two molecules in the asymmetric unit; the second molecule displayed disorder (*ca.* 13%) in the thiazine dioxide ring (see supplementary data).



Scheme 1. Synthesis of compounds **11**–**16** in the thiaplakortone tricyclic series. (a) 2-aminoethanesulfonic acid, H₂O, MeCN; (b) NaHCO_{3(aq)}, MeOH, reflux 2.5 h; (c) KOH_(aq), MeOH, O₂.

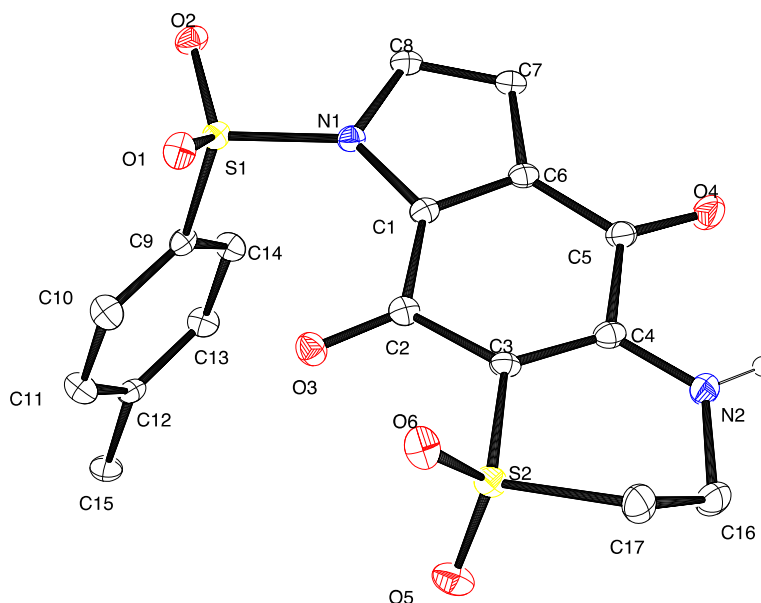


Figure 2. ORTEP diagram showing one independent molecule for compound **11**; ellipsoids are at the 30% probability level.

Subjection of the mixture of tosyl derivatives **11** and **12** to mild alkaline hydrolysis afforded a sufficient quantity of only compound **13** after purification by reversed-phase HPLC (MeOH–H₂O–0.1%TFA).

In an attempt to reverse the regioselectivity observed during the condensation of 2-aminoethanesulfonic acid with **10** and acquire suitable amounts of isomer **14**, the parent, non-tosyl protected system,

1*H*-indole-4,7-dione **17** was prepared according to literature procedures [5,8,9] and exposed to 2-aminoethanesulfinic acid. Gratifyingly, in this system, the opposite regioselectivity was observed and the respective tricyclic systems **13** and **14** were formed in a 1 to 3.3 ratio following analysis of the ¹H-NMR spectrum. Purification of this mixture by C₁₈ HPLC (MeOH-H₂O-0.1%TFA) enabled **14** to be isolated in sufficient amounts for biological testing. Oxidation of the mixture of **13** and **14** by protocols previously reported [2] afforded a mixture that was subjected to C₁₈ HPLC (MeOH-H₂O-0.1%TFA) and yielded the pure compounds **15** and **16**.

2.2. Biology and Structure-Activity Relationships

All compounds (**10–17**) were tested for *in vitro* antiplasmodial activity against chloroquine-sensitive (3D7) and multidrug-resistant (Dd2) *P. falciparum* parasite lines, and for mammalian toxicity using human neonatal foreskin fibroblast (NFF) cells. The simple indolequinones, **10** and **17**, were essentially inactive (Table 1), highlighting the importance of the 1,1-dioxo-thiazine subunit for antiplasmodial activity. The original thiaplakortone report [1] showed that unsaturation of the thiazine ring conferred enhanced antiplasmodial activity. This trend was also observed in the side-chain truncated compounds, with the unsaturated compounds, **15** and **16** displaying greater potency than their saturated counterparts, **13** and **14**, respectively. Specifically, exchanging the saturated system of **13** and **14** with the unsaturated motif present in **15** and **16** increased 3D7 activity by 23.9- and 27.3-fold, respectively; a similar SAR trend was also observed for this series towards the Dd2 line.

Table 1. Biological Data for Compounds **10–17**.

Compound	Mean IC ₅₀ ± SD (nM)			
	3D7 ^a	Dd2 ^b	NFF ^c	SI ^d
10	18,200 ± 2600	11,100 ± 4100	7600 ± 1200	0.4–0.7
11	546 ± 119	509 ± 309	1400 ± 700	2.6–2.8
12	834 ± 89	607 ± 158	19,000 ± 11,000	22.8–31.3
13	7500 ± 900	3800 ± 400	39,000 ± 4200	5.2–10.3
14	6900 ± 700	3700 ± 500	69,600 ± 5900	10.1–18.8
15	313 ± 84	129 ± 3.9	2800 ± 400	8.9–21.7
16	252 ± 35	127 ± 8.6	4600 ± 800	18.2–36.2
17	13,500 ± 6700	11,500 ± 6500	4700 ± 100	0.3–0.4
CQ ^e	7.8 ± 2.7	45 ± 10	36,500 ± 6000	811.1–4679.5

^a 3D7 = *P. falciparum* chloroquine-sensitive line; ^b Dd2 = *P. falciparum* multidrug-resistant line; ^c NFF = neonatal foreskin fibroblast cells; ^d SI = selectivity index = NFF cell-line IC₅₀/*P. falciparum* IC₅₀; ^e CQ = chloroquine (positive control).

The regiochemistry of the thiazine moiety in the original thiaplakortone report was shown to have minimal influence on the overall antiplasmodial activity and selectivity [1]. Reversal of the thiazine orientation in thiaplakortones C (**3**) and D (**4**) only showed an antiplasmodial activity increase of 1.1-fold towards both the 3D7 and Dd2 lines. In a similar manner to the earlier report, the current studies showed minimal differences in parasite potency between the side-chain truncated regioisomeric pairs, **11** and **12**, **13** and **14**, and **15** and **16**. However, when comparing NFF toxicity of the regioisomers (**11** vs. **12**; **13** vs. **14**; **15** vs. **16**) a clear trend was observed, with the thiazine regiochemistry present in **12**,

14 and **16** conveying reduced cytotoxicity ranging from 1.6- to 13.6-fold. Furthermore, the reduction in toxicity improved the selectivity indices for analogues **12**, **14** and **16**.

Biological data for compounds **11** and **12** identified that *N*-tosylation of the pyrrole moiety is well tolerated and improves antiparasitic activity, even in the absence of thiazine unsaturation. It is interesting to note that, consistent with the thiaplakortone natural products [1], the most active side-chain truncated analogues, **15** and **16**, are more potent against the drug-resistant line (Dd2) than the chloroquine-sensitive line (3D7). While it is clear that the ethylamine side-chain present in thiaplakortones A and B translates to more potent and selective antiplasmodial agents, the current study shows that the tricyclic core motif present in **11–16** represents a minimum antiplasmodial pharmacophore for the thiaplakortone chemotype.

In order to assess the drug-like properties of compounds **10–17**, *in silico* physicochemical parameters (Table 2) were calculated using ChemAxon MarvinSketch software (with calculator plugins) (<http://www.chemaxon.com>) and the data compared to Lipinski's drug-like "Rule of Five" [10]. All compounds complied with Lipinski's rules ($\text{LogP} < 5$, $\text{HBA} < 10$, $\text{HBD} < 5$, $\text{MW} < 500$). In addition, all compounds had relatively low $\text{LogD}_{7.4}$ values (except compound **10**), and had appropriate polar surface area (PSA) values for membrane penetration.

Table 2. *In silico* physicochemical parameters for compounds **10–17**^a.

Compound	MW	LogP	HBA	HBD	PSA (Å ²)	LogD _{7.4}
10	301	1.5	4	0	82	1.9
11	406	−1.6	7	1	136	−0.2
12	406	−1.6	7	1	136	−0.2
13	252	−3.3	5	2	104	−1.6
14	252	−3.3	5	2	104	−1.6
15	250	−2.9	5	2	104	−1.5
16	250	−2.9	5	2	104	−1.5
17	147	−0.2	2	1	50	0.5

^a *In silico* calculations performed using ChemAxon MarvinSketch software (with calculator plugins). MW = molecular weight (Da); HBA = H-bond acceptors; HBD = H-bond donors; PSA = polar surface area.

3. Experimental Section

3.1. General

Melting points were recorded on a capillary melting point apparatus and are uncorrected. Unless otherwise specified, ¹H and ¹³C-NMR spectra were recorded at 30 °C in DMSO-*d*₆ on a Varian INOVA 500 or 600 NMR spectrometer. The ¹H- and ¹³C-NMR chemical shifts were referenced to the solvent peak for DMSO-*d*₆ at δ_{H} 2.50 and δ_{C} 39.5. LRESIMS was obtained from LC-MS data generated using a Waters Alliance 2790 HPLC equipped with a Waters 996 photodiode array detector and an Alltech evaporative light scattering detector that was attached to a Water ZQ mass spectrometer. HRESIMS were recorded on a Bruker (Billerica, MA, USA) MicrOTof-Q spectrometer (Dionex UltiMate 3000 micro LC system, ESI mode). Analytical thin layer chromatography (TLC) was performed on aluminum-backed 0.2 mm thick silica gel 60 F₂₅₄ plates as supplied by Merck (Frankfurt, Germany). Eluted plates were visualized using a 254 nm UV lamp and/or by treatment with a suitable dip followed by heating. These dips included phosphomolybdic acid:Ce(SO₄)₂:H₂SO₄ (conc.):H₂O (37.5 g:7.5 g:

37.5 g:720 mL) or KMnO_4 : K_2CO_3 :5% NaOH aqueous solution:H₂O (3 g:20 g:5 mL:300 mL). Flash chromatographic separations were carried out following protocols defined by Still *et al.*, [11] with silica gel 60 (40–63 μm , supplied by GRACE, Baulkham Hills, NSW, Australia) or amino bonded silica gel (Davisil[®]) as the stationary phase and using the AR- or HPLC-grade solvents indicated. Semi-preparative HPLC work was performed using a Waters 600 pump and 966 PDA detector, a Gilson 715 liquid handler and a C₁₈-bonded silica Betasil 5 μm 143 Å column (21.2 mm \times 150 mm). Alltech sample preparative C₁₈-bonded silica (35–75 μm , 150 Å) and an Alltech stainless steel guard cartridge (10 mm \times 30 mm) were used for pre-adsorption and HPLC work. A Phenomenex C₁₈-bonded silica Luna 3 μm 100 Å (4.6 mm \times 50 mm) column was used for LC-MS studies. All compounds were analyzed for purity using LC-MS and shown to be >95% pure, unless otherwise stated. Starting materials and reagents were available from the Sigma-Aldrich (St. Louis, MO, USA), Merck (Frankfurt, Germany), AK Scientific Inc. (Union City, CA, USA), Matrix Scientific Chemical (Columbia, SC, USA) and were used as supplied. MeOH and CH_2Cl_2 were dried using a glass contour solvent purification system that is based upon a technology originally described by Grubbs *et al.* [12]. Where necessary, reactions were performed under a nitrogen atmosphere and glassware was heated in an oven at 140 °C then dried under vacuum prior to use. Compounds for biological studies were placed under high vacuum (0.05 mmHg) for several hours before testing to remove trace, residual solvents.

3.2. Synthesis of *N*-Tosyl Regioisomers **11** and **12**

A solution of *N*-tosyl-1*H*-indole-4,7-dione (500 mg, 1.66 mmol) in MeCN (80 mL) was treated with a solution of 2-aminoethanesulfinic acid (236 mg, 2.16 mmol) in H₂O (50 mL) in one portion. The mixture was stirred for 20 h open to the atmosphere and then H₂O was removed by rotary evaporation and the resulting solid collected by vacuum filtration. The crystals were washed with H₂O (20 mL) then dried to afford a crude ~1:11 mixture of regioisomers **12** and **11**, respectively. This material (236 mg) was pre-adsorbed to C₁₈-bonded silica (1 g) overnight, then packed into a guard cartridge that was subsequently attached to a C₁₈-bonded silica semi-preparative HPLC column. Isocratic HPLC conditions of 90% H₂O (0.1% TFA)/10% MeOH (0.1% TFA) were employed for the first 10 min, then a linear gradient to MeOH (0.1% TFA) was run over 40 min, followed by isocratic conditions of MeOH (0.1% TFA) for a further 10 min, all at a flow rate of 9 mL/min. Sixty fractions (60 \times 1 min) were collected by time from the start of the HPLC run. All UV active fractions were analyzed by ¹H-NMR spectroscopy and MS, and identical fractions were combined. This afforded **12** (7.6 mg, 1%, ^tR = 37.0–38.0 min) and **11** (69 mg, 10%, ^tR = 53.0–60.0 min). X-ray quality crystals of **11** were obtained through slow evaporation using a H₂O/MeOH (1:9) mix.

Compound **11**: Dull orange crystals (H₂O/MeOH); mp > 300 °C; ¹H-NMR (600 MHz, DMSO-*d*₆) δ_{H} 2.42 (3H, s, H-15), 3.27–3.29 (2H, m, H-2), 3.76–3.78 (2H, m, H-3), 6.83 (1H, d, J = 3.4 Hz, H-6), 7.50 (2H, d, J = 8.2 Hz, H-13), 7.90 (2H, d, J = 3.4 Hz, H-7), 8.01 (2H, d, J = 8.2 Hz, H-12), 9.01 (1H, br s, H-4); ¹³C-NMR (150 MHz, DMSO-*d*₆) δ_{C} 21.2 (C-15), 39.3 (C-3), 48.2 (C-2), 107.5 (C-6), 108.2 (C-9a), 126.7 (C-5a), 128.6 (2C, C-12), 129.3 (C-7), 129.8 (2C, C-13), 130.8 (C-8a), 133.5 (C-11), 146.2 (C-14), 146.6 (C-4a), 167.1 (C-9), 175.1 (C-5); (+)-LRESIMS m/z (rel. int.) 407 (100) [M + H]⁺; (–)-LRESIMS m/z (rel. int.) 405 (100) [M – H][–]; (+)-HRESIMS m/z 429.0200 [M + Na]⁺ (calcd for C₁₇H₁₄N₂NaO₆S₂, 429.0185).

Compound **12**: Bright orange amorphous solid; $^1\text{H-NMR}$ (600 MHz, $\text{DMSO-}d_6$) δ_{H} 2.41 (3H, s, H-15), 3.26–3.28 (2H, m, H-2), 3.75–3.77 (2H, m, H-3), 6.81 (1H, d, $J = 3.2$ Hz, H-8), 7.48 (2H, d, $J = 8.4$ Hz, H-13), 7.98 (2H, d, $J = 8.4$ Hz, H-12), 8.12 (2H, d, $J = 3.2$ Hz, H-7), 9.13 (1H, br s, H-4); $^{13}\text{C-NMR}$ (150 MHz, $\text{DMSO-}d_6$) δ_{C} 21.1 (C-15), 39.2 (C-3), 47.9 (C-2), 108.0 (C-9a), 108.8 (C-8), 125.9 (C-8a), 128.3 (2C, C-12), 130.0 (2C, C-13), 133.1 (C-11), 133.2 (C-7), 133.3 (C-5a), 146.4 (C-14), 147.4 (C-4a), 166.3 (C-5), 172.9 (C-9); (–)-LRESIMS m/z (rel. int.) 405 (100) $[\text{M} - \text{H}]^-$; (+)-LRESIMS m/z (rel. int.) 407 (100) $[\text{M} + \text{H}]^+$; (+)-HRESIMS m/z 429.0167 $[\text{M} + \text{Na}]^+$ (calcd for $\text{C}_{17}\text{H}_{14}\text{N}_2\text{NaO}_6\text{S}_2$, 429.0185).

3.3. Deprotection of the *N*-Tosyl Regioisomer Mixture to Yield **13**

A 1:11 mixture of **12** and **11** (140 mg, 0.35 mmol) in a saturated solution of NaHCO_3 (5 mL) and MeOH (50 mL) was heated to reflux for 2.5 h. The mixture was acidified with HCl (32% aqueous) to pH 6 then concentrated and subjected to flash chromatography (silica, 1:10 *v/v* MeOH/ CH_2Cl_2 elution) to afford a 1:26 mixture of compounds **14** and **13** (59 mg, 68%). This material (59 mg) was pre-adsorbed to C_{18} -bonded silica (1 g) overnight, then packed into a guard cartridge that was attached to a C_{18} -bonded silica semi-preparative HPLC column. Application of the same reversed-phase HPLC purification method described above (Section 3.2) afforded **13** (15 mg, 11%, $^1\text{R} = 23.0$ – 24.0 min) as an orange powder.

Compound **13**: Orange amorphous solid; $^1\text{H-NMR}$ (500 MHz, $\text{DMSO-}d_6$) δ_{H} 3.31–3.33 (2H, m, H-2), 3.81–3.84 (2H, m, H-3), 6.57 (1H, d, $J = 2.8$ Hz, H-6), 7.13 (1H, d, $J = 2.8$ Hz, H-7), 9.05 (1H, brs, H-4), 12.76 (1H, brs, H-8); $^{13}\text{C-NMR}$ (125 MHz, $\text{DMSO-}d_6$) δ_{C} 39.4 (C-3), 48.2 (C-2), 107.5 (C-6), 120.7 (C-5a), 125.4 (C-7), 132.9 (C-8a), 148.2 (C-4a), 169.8 (C-9), 174.1 (C-5); (+)-LRESIMS m/z (rel. int.) 253 (100) $[\text{M} + \text{H}]^+$; (–)-LRESIMS m/z (rel. int.) 251 (100) $[\text{M} - \text{H}]^-$; (+)-HRESIMS m/z 275.0104 $[\text{M} + \text{Na}]^+$ (calcd for $\text{C}_{10}\text{H}_8\text{N}_2\text{NaO}_4\text{S}$, 275.0097).

3.4. Synthesis of Regioisomers **13** and **14**

A solution of 1*H*-indole-4,7-dione (**10**, 504 mg, 3.4 mmol) in MeCN (160 mL) was treated with a solution of 2-aminoethanesulfinic acid (482 mg, 4.42 mmol) in H_2O (50 mL) in one portion and the mixture stirred for 20 h under an atmosphere of O_2 . The MeCN and H_2O were removed by rotary evaporation to afford an orange solid, which was purified by flash chromatography (silica, 1:5 *v/v* MeOH/ CH_2Cl_2 elution) to afford a 3.3:1 mixture of regioisomers **14** and **13**, respectively (307 mg, 36%). A portion of this material (40 mg) was pre-adsorbed to C_{18} -bonded silica (1 g) overnight, then packed into a guard cartridge that was attached to a C_{18} -bonded silica semi-preparative HPLC column. Isocratic HPLC conditions of 95% H_2O (0.1% TFA)/5% MeOH (0.1% TFA) were employed for the first 10 min, then a linear gradient to 50% H_2O (0.1% TFA)/50% MeOH (0.1% TFA) was run over 40 min, followed by a linear gradient to MeOH (0.1% TFA) in 1 min, then isocratic conditions of MeOH (0.1% TFA) for a further 9 min, all at a flow rate of 9 mL/min. Sixty fractions (60 \times 1 min) were collected by time from the start of the HPLC run. All UV active fractions were analyzed by $^1\text{H-NMR}$ spectroscopy and MS, and identical fractions were combined. This yielded **14** (5.0 mg, 1%, $^1\text{R} = 25.0$ – 27.0 min) as a bright orange powder.

Compound **14**: Bright orange amorphous solid; $^1\text{H-NMR}$ (500 MHz, $\text{DMSO-}d_6$) δ_{H} 3.28–3.33 (2H, m, H-2), 3.79–3.82 (2H, m, H-3), 6.53 (1H, d, $J = 2.5$ Hz, H-8), 7.40 (1H, d, $J = 2.5$ Hz, H-7), 8.89 (1H,

br s, H-4), 12.81 (1H, br s, H-6); ^{13}C -NMR (125 MHz, DMSO- d_6) δ_{C} 39.3 (C-3), 48.4 (C-2), 108.4 (2C, C-9a, C-8), 127.2 (C-8a), 128.2 (C-5a), 130.1 (C-7), 147.5 (C-4a), 167.9 (C-5), 174.7 (C-9); (+)-LRESIMS m/z (rel. int.) 253 (100) $[\text{M} + \text{H}]^+$; (-)-LRESIMS m/z (rel. int.) 251 (100) $[\text{M} - \text{H}]^-$; (+)-HRESIMS m/z 275.0087 $[\text{M} + \text{Na}]^+$ (calcd for $\text{C}_{10}\text{H}_8\text{N}_2\text{NaO}_4\text{S}$, 275.0097).

3.5. Synthesis of Regioisomers 15 and 16

A 3.3:1 regioisomeric mixture of **14** and **13** (90 mg, 0.36 mmol) from the synthesis described above (Section 3.4) in a solution of MeOH (10 mL) was treated with an aqueous KOH solution (6 mL, 12 M). The magnetically stirred reaction mixture was purged with O_2 , and maintained at 60 °C under a balloon of O_2 for 4 h. The reaction mixture was cooled to 0 °C, carefully neutralized by the addition of an aqueous solution of HCl (1 M) and then the mixture was concentrated *in vacuo* to afford a residue that was subjected to flash chromatography through a small plug of silica (1:10 v/v MeOH/ CH_2Cl_2 elution) and after concentration of the eluent *in vacuo*, the residue (40 mg) was pre-adsorbed to C_{18} -bonded silica (1 g) overnight, then packed into a guard cartridge that was attached to a C_{18} -bonded silica semi-preparative HPLC column. Application of same reversed-phase HPLC purification method described above (section 3.4) resulted in the purification of compounds **16** (15 mg, 17%, t_{R} = 28.0–30.0 min) and **15** (5 mg, 6%, t_{R} = 32.0–34.0 min) as yellow and orange powders, respectively.

Compound **15**: Orange amorphous solid; ^1H -NMR (500 MHz, DMSO- d_6) δ_{H} 6.49 (1H, d, J = 8.8 Hz, H-2), 6.66 (1H, d, J = 2.8 Hz, H-6), 7.07 (1H, d, J = 8.8 Hz, H-3), 7.27 (1H, d, J = 2.8 Hz, H-7), 11.07 (1H, br s, H-4), 12.99 (1H, br s, H-8); ^{13}C -NMR (125 MHz, DMSO- d_6) δ_{C} 108.0 (C-6), 111.7 (C-2), 113.4 (C-9a), 121.8 (C-5a), 126.8 (C-7), 130.2 (C-3), 131.3 (C-8a), 140.5 (C-4a), 172.2 (C-9), 174.1 (C-5); (+)-LRESIMS m/z (rel. int.) 251 (100) $[\text{M} + \text{H}]^+$; (-)-LRESIMS m/z (rel. int.) 249 (100) $[\text{M} - \text{H}]^-$; (+)-HRESIMS m/z 272.9939 $[\text{M} + \text{Na}]^+$ (calcd for $\text{C}_{10}\text{H}_6\text{N}_2\text{NaO}_4\text{S}$, 272.9940).

Compound **16**: Yellow amorphous solid; ^1H NMR (500 MHz, DMSO- d_6) δ_{H} 6.42 (1H, d, J = 8.8 Hz, H-2), 6.60 (1H, d, J = 2.6 Hz, H-8), 7.04 (1H, d, J = 8.8 Hz, H-3), 7.43 (1H, d, J = 2.6 Hz, H-7), H-4 and H-6 not observed; ^{13}C -NMR (125 MHz, DMSO- d_6) δ_{C} 108.5 (C-8), 111.6 (C-2), 113.9 (C-9a), 126.9 (C-8a), 127.6 (C-5a), 129.8 (C-7), 130.1 (C-3), 140.2 (C-4a), 167.9 (C-5), 177.3 (C-9); (+)-LRESIMS m/z (rel. int.) 251 (100) $[\text{M} + \text{H}]^+$; (-)-LRESIMS m/z (rel. int.) 249 (100) $[\text{M} - \text{H}]^-$; (+)-HRESIMS m/z 272.9933 $[\text{M} + \text{Na}]^+$ (calcd for $\text{C}_{10}\text{H}_6\text{N}_2\text{NaO}_4\text{S}$, 272.9940).

3.6. X-ray Crystallography Studies on Compound 11

Intensity data were collected with an Oxford Diffraction SuperNova CCD diffractometer using Cu-K α radiation, the temperature during data collection was maintained at 100.0(1) using an Oxford Cryosystems cooling device. The structure was solved by direct methods and difference Fourier Synthesis [13]. Hydrogen atoms bound to the carbon atom were placed at their idealized positions using appropriate HFIX instructions in SHELXL, and included in subsequent refinement cycles. Hydrogen atoms attached to nitrogen were located from difference Fourier maps and refined freely with isotropic displacement parameters. Thermal ellipsoid plots were generated using the program ORTEP-3 [14] integrated within the WINGX suite of programs [15]. Full details of the data collection and refinement and tables of atomic coordinates, bond lengths and angles, and torsion angles have been deposited with

the Cambridge Crystallographic Data Centre (CCDC 1416796). Copies can be obtained free of charge on application at the following address: <http://www.ccdc.cam.ac.uk>.

Crystal data for compound **11**: C₁₇H₁₄N₂O₆S₂, $M = 406.42$, $T = 100.0(2)$ K, $\lambda = 1.5418$ Å, Triclinic, space group $P2_1/c$, $a = 11.6802(7)$, $b = 28.0975(14)$, $c = 10.3047(6)$ Å, $\beta = 91.539(5)^\circ$ $V = 3380.6(3)$ Å³, $Z = 8$, $Z' = 2$, $D_c = 1.597$ Mg·M⁻³, $\mu = 3.230$ mm⁻¹, $F(000) = 1680$, crystal size 0.49 mm × 0.38 mm × 0.31 mm. $\theta_{\max} = 67.6^\circ$, 10,831 reflections measured, 5907 independent reflections ($R_{\text{int}} = 0.051$) the final $R = 0.0559$ [$I > 2\sigma(I)$, 5134 data] and $wR(F^2) = 0.1577$ (all data) GOOF = 1.027.

3.7. *P. falciparum* Growth Inhibition Assay

P. falciparum growth inhibition assays were carried out using an isotopic microtest, as previously described [16]. Briefly, *in vitro* cultured *P. falciparum* infected erythrocytes (1.0% parasitemia and 1.0% hematocrit) were seeded into triplicate wells of 96 well tissue culture plates containing vehicle control (DMSO), positive control [chloroquine (Sigma-Aldrich, St. Louis, MO, USA), catalogue #C6628, >98%] or test compounds and incubated under standard *P. falciparum* culture conditions with 0.5 µCi [³H]-hypoxanthine. The final concentration of DMSO vehicle was <0.5% in all assay wells (non-toxic). After 48 h cells were harvested onto 1450 MicroBeta filter mats (PerkinElmer, Waltham, Massachusetts, USA) and [³H] incorporation determined using a 1450 MicroBeta liquid scintillation counter. Percentage inhibition of growth compared to matched DMSO controls was determined and IC₅₀ values were calculated using linear interpolation of inhibition curves [17]. The mean IC₅₀ or % inhibition (±SD) was calculated for three independent experiments, each carried out in triplicate.

4. Conclusions

In summary, six analogues associated with the tricyclic core of thiaplakortones were synthesized from readily accessible and known 1*H*-indole-4,7-dione derivatives, and isolated in low to moderate yields. Regiochemistry was moderated by substitution of the indole nitrogen. All compounds were tested for *in vitro* antiplasmodial activity towards two *P. falciparum* parasite lines (3D7 and Dd2). Compound **16** showed the best antiparasitic activity with IC₅₀ values of 252 and 127 nM towards 3D7 and Dd2 lines, respectively. The moderate toxicity (IC₅₀ 4600 nM) of compound **16** towards NFF cells equates to a selectivity index of 18.2–36.2. These studies have identified that while the ethylamine side-chain present in the marine natural products, thiaplakortones A and B, translates to more potent and selective antiplasmodial compounds, this functionality is by no means essential for activity. Furthermore, the truncated thiaplakortone molecules (**11–16**) synthesized during this work has allowed delineation of a minimum antiplasmodial pharmacophore for the thiaplakortone chemotype.

Acknowledgments

We thank the National Health and Medical Research Council (NHMRC) for financial support towards this research through a project grant (APP1024314). R.A.D. and K.T.A. acknowledge the Australian Research Council (ARC) for an ARC Linkage Grant (LP120200339) and an ARC Future Fellowship, respectively. We also thank the ARC for support toward NMR and MS equipment (Grant LE0668477 and LE0237908). G. MacFarlane (University of Queensland) and W. Loa (Griffith University) are

acknowledged for HRESIMS measurements. We also acknowledge the Australian Red Cross Blood Service for the provision of human blood and sera.

Author Contributions

B.D.S. designed and conducted all synthetic experiments and analyzed the results. T.S.S. and K.T.A. designed and performed all the biological experiments, and contributed to data interpretation. M.J.C. assisted with synthetic experimental design, and SAR data analysis. J.M.W. obtained the X-ray diffraction data for compound **11**, and solved the crystal structure. R.A.D. was the project leader overseeing the design of the experiments, analysis of the results and the identification and characterization of all compounds. All authors contributed to manuscript preparation.

Conflicts of Interest

The authors declare no conflict of interest.

References

1. Davis, R.A.; Duffy, S.; Fletcher, S.; Avery, V.M.; Quinn, R.J. Thiaplakortones A-D: Antimalarial Thiazine Alkaloids from the Australian Marine Sponge *Plakortis lita*. *J. Org. Chem.* **2013**, *78*, 9608–9613.
2. Pouwer, R.H.; Deydier, S.M.; Le, P.V.; Schwartz, B.D.; Franken, N.C.; Davis, R.A.; Coster, M.J.; Charman, S.A.; Edstein, M.D.; Skinner-Adams, T.S.; *et al.* Total Synthesis of Thiaplakortone A: Derivatives as Metabolically Stable Leads for the Treatment of Malaria. *ACS Med. Chem. Lett.* **2013**, *5*, 178–182.
3. Schwartz, B.; Skinner-Adams, T.; Andrews, K.T.; Coster, M.; Edstein, M.; MacKenzie, D.; Charman, S.; Koltun, M.; Blundell, S.; Campbell, A.; *et al.* Synthesis and antimalarial evaluation of amide and urea derivatives based on the thiaplakortone A natural product scaffold. *Org. Biomol. Chem.* **2015**, *13*, 1558–1570.
4. Hollis Showalter, H.D.; Pohlmann, G. An Improved Synthesis of 4,7-Dimethoxy-1*H*-Indole. *Org. Prep. Proc. Int.* **1992**, *24*, 484–488.
5. Jackson, Y.A.; Billimoria, A.D.; Sadanandan, E.V.; Cava, M.P. Regioselective Amination of Indole-4,7-quinones. *J. Org. Chem.* **1995**, *60*, 3543–3545.
6. Rajeswari, S.; Drost, K.J.; Cava, M.P. A convenient reductive cyclization of β ,2-dinitrostyrenes to indoles. *Heterocycles* **1989**, *29*, 415.
7. Schmitz, F.J.; Bloor, S.J. Xesto- and halenaquinone derivatives from a sponge, *Adocia* sp., from Truk lagoon. *J. Org. Chem.* **1988**, *53*, 3922–3925.
8. Cherif, M.; Cotelle, P.; Catteau, J.P. General synthesis of 2,3-substituted 5-membered heterocyclic quinones. *Heterocycles* **1992**, *34*, 1749–1758.
9. Kitahara, Y.; Nakahara, S.; Numata, R.; Kubo, A. Synthesis of 4,7-Indolequinones. The Oxidative Demethylation of 4,7-Dimethoxyindoles with Ceric Ammonium Nitrate. *Chem. Pharm. Bull.* **1985**, *33*, 2122–2128.

10. Lipinski, C.A.; Lombardo, F.; Dominy, B.W.; Feeney, P.J. Experimental and computational approaches to estimate solubility and permeability in drug discovery and development settings. *Adv. Drug Deliv. Rev.* **2001**, *46*, 3–26.
11. Still, W.C.; Kahn, M.; Mitra, A. Rapid chromatographic technique for preparative separations with moderate resolution. *J. Org. Chem.* **1978**, *43*, 2923–2925.
12. Pangborn, A.B.; Giardello, M.A.; Grubbs, R.H.; Rosen, R.K.; Timmers, F.J. Safe and Convenient Procedure for Solvent Purification. *Organometallics* **1996**, *15*, 1518–1520.
13. Sheldrick, G.M. A short history of SHELX. *Acta Cryst.* **2008**, *A64*, 112–122.
14. Farrugia, L.J. ORTEP-3 for windows—A version of ORTEP-III with a graphical user interface (GUI). *J. Appl. Cryst.* **1997**, *30*, 565.
15. Farrugia, L.J. WinGX suite for small-molecule single-crystal crystallography. *J. Appl. Cryst.* **1999**, *32*, 837–838.
16. Skinner, T.S.; Manning, L.S.; Johnston, W.A.; Davis, T.M. E. *In vitro* stage-specific sensitivity of *Plasmodium falciparum* to quinine and artemisinin drugs. *Int. J. Parasitol.* **1996**, *26*, 519–525.
17. Huber, W.; Koella, J.C. A comparison of three methods of estimating EC₅₀ in studies of drug resistance of malaria parasites. *Acta Trop.* **1993**, *55*, 257–261.

© 2015 by the authors; licensee MDPI, Basel, Switzerland. This article is an open access article distributed under the terms and conditions of the Creative Commons Attribution license (<http://creativecommons.org/licenses/by/4.0/>).